Pergamon

Scripta Materialia, Vol. 37, No. 5, pp. 707–712, 1997
Elsevier Science Ltd

1359-6462/97 $17.00 + .00

PII S1359-6462(97)00154-1

ON THE GROWTH OF SMALL FATIGUE CRACKS IN γ-BASED TITANIUM ALUMINIDES

J.P. Campbell, J.J. Kruzic, S. Lillibridge, K.T. Venkateswara Rao* and R.O. Ritchie
Department of Materials Science and Mineral Engineering,
University of California at Berkeley, Berkeley, CA 94720-1760

(Received February 20, 1997)
(Accepted March 24, 1997)

Introduction

Gamma-based TiAl intermetallic alloys have received considerable attention recently as candidate materials for high-temperature aerospace applications (1-4). Two classes of microstructure have been prominent in the two-phase ($\gamma + \alpha_2$) alloys: a lamellar structure consisting of lamellar colonies containing alternating γ and α_2 platelets, and a duplex structure consisting of equiaxed grains of γ with small amounts of α_2 grains (1). In general, duplex structures display better elongation and strength, whereas lamellar structures show better toughness and fatigue crack-growth resistance (2,5-8). However, a problem with both microstructures, as with most intermetallics, is that fatigue-crack growth rates, da/dN, show a very strong dependence upon the applied stress-intensity range, ΔK, i.e., $da/dN \propto \Delta K^m$, where m is greater than ~10 (11,12). With such high exponents, predicted component lives based on damage-tolerant analyses are often unacceptably sensitive to applied stress levels, necessitating that the applied ΔK levels remain below a fatigue threshold, ΔK_{TH}. In the presence of "small cracks", however, this approach may be non-conservative.

Small cracks (typically < ~500 μm in length) are known to grow at applied ΔK below the "long crack" threshold, and to exhibit growth rates in excess of those corresponding to long cracks (typically larger than 2-3 mm) at the same *applied* ΔK levels (11-14). Such effects are apparent when crack sizes become comparable to i) the characteristic microstructural dimensions (a continuum limitation), ii) the extent of local inelasticity (i.e., the plastic-zone size) *ahead* of the crack tip (a linear-elastic fracture mechanics limitation), or iii) the extent of the zone of crack-tip shielding *behind* the crack tip (a similitude limitation). Accordingly, the objective of the present study is to examine the small-crack effect in a commercial γ-based TiAl alloy by comparing the growth-rate behavior of long (through-thickness) cracks with that of small surface cracks for both duplex and fully lamellar microstructures.

Materials and Experimental Procedures

The TiAl alloy studied, of nominal composition (at.%) Ti-47Al-2Nb-2Cr-0.2B, contained B additions which resulted in ~0.5 vol.% of needle-like TiB_2 particles (~2-10 μm in length and ~1 μm in diameter).

*Currently at Advanced Cardiovascular Systems, Guidant Corporation, 3200 Lakeside Drive, Santa Clara, CA 95052

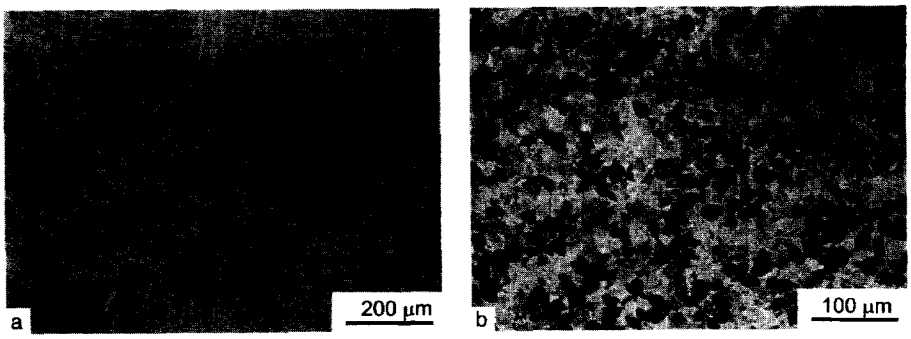

Figure 1. Optical micrographs of the (a) lamellar and (b) duplex microstructures in Ti-47Al-2Nb-2Cr-0.2B (at.%). Etchant: aqueous 2% HF/ 5% H_3PO_4.

The lamellar microstructure was obtained by a two-step forging process, followed by heat treating in flowing argon gas at 1370°C for 1 hr, air cooling and then holding 6 hr at 900°C prior to argon gas furnace cooling. The resulting microstructure featured ~145 μm-sized lamellar colonies with very small amounts (~4%) of fine equiaxed γ grains (5-20 μm) between lamellar colonies; the α_2 layer (center-to-center) spacing was ~1.3 μm (Fig. 1a). The duplex microstructure was achieved through a furnace cool after heat treating the forged alloy at 1320°C for 3 hr in argon. The structure consisted of nearly equiaxed grains of the γ-phase, ~17 μm in diameter (Fig. 1b), with ~10 vol.% α_2 present in the form of thin layers (~1-3 μm thick) at grain boundaries or as larger "blocky" regions (~3-23 μm in diameter) at triple points. A small proportion of fine lamellar colonies was also present.

Long (>5 mm) crack growth rates were measured on through-thickness cracks using 4-mm thick compact-tension, C(T), specimens. Tests were conducted in 25°C air at 25 Hz (sine wave) in accordance with ASTM Standard E647; a load ratio, R, of 0.1 ($= K_{min}/K_{max}$) was maintained. Fatigue thresholds, ΔK_{TH}, operationally defined as the applied ΔK below which da/dN $<10^{-10}$ m/cycle, were approached using a variable-ΔK/constant-R load-shedding scheme. Crack lengths were monitored using electrical-potential measurements (on NiCr foil gauges bonded to the side face of the specimen) and using back-face strain compliance.

Elastic compliance data were also utilized to measure the extent of crack-tip shielding from crack closure and crack bridging. Crack closure was evaluated in terms of the closure stress intensity, K_{cl}, which was approximately defined at the load corresponding to first deviation from linearity on the unloading compliance curve (15,16). Crack bridging was assessed through a comparison of the experimentally measured unloading compliance (at loads above those associated with closure) with the theoretical value for a traction-free crack (17). With this technique, a bridging stress intensity, K_{br}, representing the reduction in K_{max} due to the bridging tractions developed in the crack wake, was estimated.

Small (c < 300 μm) crack growth rates were investigated using unnotched rectangular beams (of width 10 mm, thickness 6 mm, and span 50 mm), loaded in four-point bending. Small surface cracks associated with electro-discharge machining (EDM) pit damage were cyclically loaded to grow the cracks away from the EDM heat-affected zone (HAZ) prior to data acquisition (HAZ was identified optically using an aqueous 2% HF, 5% H_3PO_4 etchant on a polished surface). In some instances, sample surfaces were ground and polished following pitting to completely eliminate the HAZ, leaving only small cracks on the surface. Using this procedure, initial surface flaws with half lengths less than c ~125 μm were achieved.

Bend samples were cycled at R = 0.1 between 5 and 25 Hz (sine wave), with crack lengths monitored by periodic surface replication using cellulose acetate tape. Replicas were Au or Pt coated to

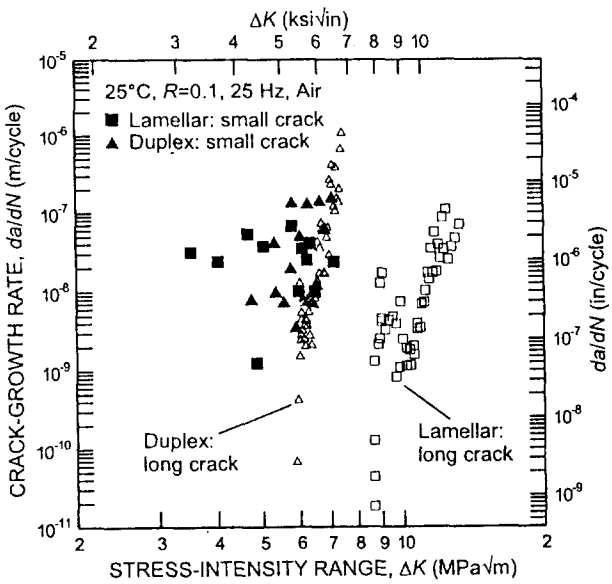

Figure 2. Fatigue crack-growth rates for through-thickness long cracks ($a > 5$ mm) and small surface cracks ($c \sim 35$-275 μm) in the lamellar and duplex microstructures of Ti-47Al-2Nb-2Cr-0.2B. Small-crack data points represent average growth rates over a specific increment of crack extension (between two surface replications).

improve resolution prior to optical measurement of crack lengths. Average growth rates were computed from the amount of crack extension between two discrete measurements. Stress intensities were determined using linear-elastic solutions for surface cracks in bending (18), assuming a semi-circular crack profile (crack depth to half surface crack length ratio, $a/c = 1$). This assumption was verified by heat tinting select samples at 600°C for 4 hr prior to fracture to measure the crack shape; measurements revealed an average a/c ratio of 1.04 which corresponds to a semi-circular crack.

Results and Discussion

Figure 2 shows the fatigue-crack growth rates of through-thickness long cracks in the lamellar and duplex microstructures. Growth rates are clearly a strong function of ΔK, with Paris power-law exponents, m, in the mid-growth-rate regime ranging from 9 in the lamellar to 22 in the duplex structure. Crack-growth resistance is considerably greater in the lamellar structure; indeed growth rates (at a specific ΔK) are up to five orders of magnitude lower and threshold ΔK_{TH} values ~1½ times larger than in the duplex material, resulting from a significant role of crack-tip shielding (4,8,19). Under monotonic loading, inter- and intra-lamellar microcracking ahead of the crack tip results in the development of uncracked ("shear") ligament bridges in the crack wake (20,21). Crack bridging by these ligaments is the principal mechanism of toughening in the lamellar microstructure (20), with a bridging stress intensity K_{br} on the order of 12 MPa√m (19). No such bridging is seen in the duplex material. Under cyclic loading in the lamellar structure, the bridging is diminished in part due to fatigue failure of the ligaments; nevertheless, it still has a prominent effect (19), i.e., K_{br} values in fatigue have been measured as high as 2 MPa√m (14% of K_{max}) at $\Delta K \sim 13$ MPa√m. In addition, the resulting meandering crack paths promote (roughness-induced) crack closure from the wedging of asperities (19). Although the interpretation of closure measurements can be somewhat uncertain in the presence of bridging,

measured K_{cl} values at $R = 0.1$ ranged from ~4-7 MPa$\sqrt{m}$ in the lamellar structure to ~1.6-2.2 MPa$\sqrt{m}$ in the duplex structure.

Corresponding results for the growth of cracks with half surface lengths between ~35-275 μm are plotted in Fig. 2. Clearly, small-crack growth rates have characteristically far greater scatter than long-crack data, associated with a biased sampling of the microstructure by flaws which are comparable in size with microstructural dimensions (22). Moreover, in marked contrast to long-crack behavior, the scatter bands for the lamellar and duplex microstructures essentially overlap, although crack growth in the lamellar structure occurs at slightly lower ΔK levels. The most significant results, however, are that, at equivalent applied ΔK levels, small-crack growth rates exceed those of corresponding long cracks by up to 3 orders of magnitude, and crack growth is observed in both structures at applied ΔK levels well below the long-crack threshold, ΔK_{TH}. Specifically, small-crack growth is evident at applied ΔK levels as low as 3.5 and 4.7 MPa$\sqrt{m}$ in the lamellar and duplex structures, respectively; corresponding long-crack thresholds are, respectively, 8.6 and 6.0 MPa$\sqrt{m}$. Differences between long- and small-crack behavior, however, are much reduced in the duplex microstructure.

Given the salient role of shielding in the crack-growth resistance of γ-based TiAl alloys, in particular for the lamellar microstructure, it is likely that small flaws in these alloys will be susceptible to a *similitude limitation.* In other words, by virtue of their limited wake, they do not develop equilibrium zones of crack-tip shielding akin to long cracks. Such shielding, which arises primarily from uncracked ligament bridging and roughness-induced crack closure, is much less prominent in the duplex structure, consistent with the minimal difference in small- and long-crack data in this microstructure. Indeed, since the superior long fatigue crack-growth properties of lamellar microstructures have been principally attributed to shielding mechanisms (19), the similar fatigue crack-growth properties of the duplex and lamellar structures for small-crack sizes would appear to result from a reduced shielding contribution at these crack sizes. The limited role of such shielding during small-crack growth and the observed similarity of the duplex and lamellar small-crack data thus implies that there is little difference in *intrinsic* fatigue crack-growth resistance of the two microstructures.

To verify this similitude limitation quantitatively, the shielding contributions from both uncracked ligament bridging and crack closure were experimentally measured and "subtracted" from the long crack results on the assumption that the effective (local) driving force at the crack tip, ΔK_{eff}, can be described (for $K_{cl} > K_{min}$) by:

$$\Delta K_{eff} = (K_{max} - K_{br}) - K_{cl}. \quad (1)$$

Here K_{br} is the bridging stress intensity associated with bridging tractions developed across the crack flank, and K_{cl} is the closure stress intensity, arising primarily from the wedging of fracture-surface asperities inside the crack. Specific measurements of K_{br} and K_{cl} are documented in ref. 19; results in terms of their effect on the normalization of long- and small-crack data are shown respectively in Figs. 3a and b for the lamellar and duplex microstructures.

As illustrated in Fig. 3, replotting the long-crack data in terms of ΔK_{eff} after correcting for bridging and closure results in a far closer correspondence between the long and small crack behavior, although the normalization is less effective for the lamellar microstructure where small-crack growth is evident at stress intensities below the $\Delta K_{TH,eff}$ threshold. This is, however, to be expected because crack sizes are comparable to the scale of the coarser lamellar microstructure (*continuum limitation*). For crack sizes smaller than the grain size, the crack front of the elliptical flaw at most sampled only a few lamellar colonies. Prior studies of the effect of lamellar orientation on fatigue crack-growth rates have indicated that growth rates are faster when cracking is coplanar with the lamellar (γ/α_2) interface, particularly at low ΔK levels (23-26). It is thus unlikely that a continuum parameter such as the long-

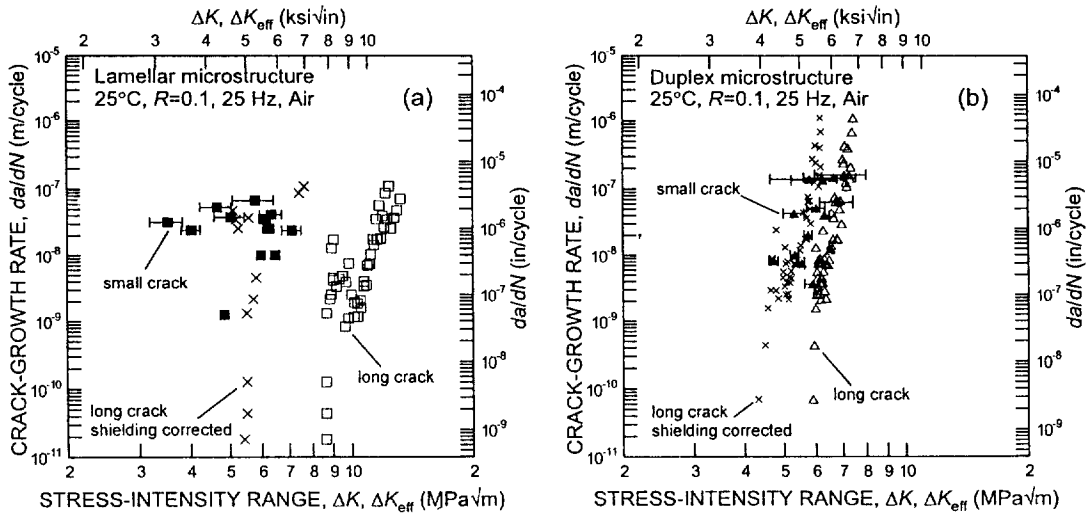

Figure 3. Comparison of long-crack, small-crack, and shielding corrected long-crack fatigue data in the (a) lamellar and (b) duplex microstructures. Growth rates, da/dN, for the shielding corrected data are plotted as a function of ΔK_{eff} after allowing for the effect of both crack bridging and closure (see text). Error bars on the small crack data represent the range of ΔK over the increment of measured crack growth.

crack threshold, which is determined for a large crack which samples many lamellar colonies, would reflect the worst-case growth-rate behavior of a small crack confined to only one or two colonies.

In terms of the potential use of γ-TiAl alloys in fatigue-critical situations, the present data suggest a somewhat surprising result that the duplex microstructure may offer the better properties and be more amenable to reliable application in damage-tolerant design. Indeed, although the scatter bands for the two alloys largely overlap, the lamellar structure exhibits small-crack growth at lower ΔK levels. Moreover, as design may have to be based on a fatigue threshold due to the steep exponents in the (long) crack-growth law, the ability to define a lower-bound threshold value will be critical. The definition of such limits appears feasible for duplex microstructures in terms of (a shielding-corrected) $\Delta K_{TH,eff}$ threshold, at least for crack sizes larger than characteristic microstructural dimensions (~20 μm). In contrast, it is more difficult to define a similar threshold for the lamellar structures as characteristic microstructural dimensions are up to an order of magnitude larger. Accordingly, the growth rates of small fatigue cracks up to $c \sim 300$ μm in length show considerable scatter due to statistical sampling of the microstructure, and continue to propagate at stress intensities below the $\Delta K_{TH,eff}$ threshold.

Conclusions

Based on an experimental study of the fatigue-crack growth behavior of long (>5 mm) through-thickness and small ($c < 300$ μm) surface cracks in duplex and lamellar microstructures in a Ti-47Al-2Nb-2Cr-0.2B (at.%) alloy at 25°C, the following conclusions can be made:

1. Small-crack growth rates in both microstructures are faster than those of corresponding long cracks at the same applied ΔK levels; moreover, small cracks are found to propagate at applied ΔK levels below the long-crack threshold ΔK_{TH}.
2. This effect is primarily attributed to the role of crack-tip shielding, principally from uncracked ligament bridging and crack closure, in impeding long-crack growth rates (similitude limitation), as closer correspondence between long- and small-crack data is achieved after "correcting" for

such shielding. Small-crack growth, however, is still evident below this lower-bound threshold in lamellar structures even after such normalization, due to statistical sampling of the coarser microstructure (continuum limitation).

3. A comparison of long-crack data suggest that the fatigue crack-growth resistance of the lamellar structure is significantly greater than that of the duplex structure, with growth rates being up to five orders of magnitude lower at equivalent ΔK levels. A comparison of small-crack data, conversely, indicates marginally superior fatigue crack-growth resistance in the duplex structure (although the scatter bands for the two structures overlap).
4. Duplex microstructures appear to offer better properties from the perspective of their potential use in fatigue-critical applications. In addition to their higher strength and ductility, the definition of a shielding-corrected (lower-bound) $\Delta K_{TH,eff}$ threshold, below which both small- and long-cracks are dormant, appears feasible. Such an approach is less certain for the coarser lamellar microstructures where small cracks of grain-size dimensions continue to propagate below this lower-bound threshold (a continuum limitation).

Acknowledgments

This work was funded by the Air Force Office of Scientific Research under Grant F49620-96-1-0233. We thank Dr. D.S. Shih (McDonnell-Douglas) for supplying the alloys, the Office of Naval Research for a NDSEG Fellowship (for JPC), and Dr. C.H. Ward for his support.

References

1. Y.-W. Kim, *J. Metals*, **46:7**, 30 (1994).
2. Y.-W. Kim and D.M. Dimiduk, *J. Metals*, **43:8**, 40 (1991).
3. G.F. Harrison and M.R. Winstone, in *Mechanical Behaviour of Materials at High Temperature*, eds. C.M. Branco, R.O. Ritchie and V. Sklenicvka, Kluwer, 309 (1996).
4. J.M. Larsen, B.D. Worth, S.J. Balsone and J.W. Jones, in *Gamma Titanium Aluminides*, eds. Y.-W. Kim *et al.*, TMS, Warrendale, PA, 821 (1995).
5. K S. Chan, *Metall. Trans. A*, **24**, 569 (1993).
6. K.S. Chan and Y.-W. Kim, *Metall. Trans. A*, **23**, 1663 (1992).
7. K.S. Chan and Y.-W. Kim, *Metall. Trans. A*, **24**, 113 (1993).
8. K.T. Venkateswara Rao, Y.-W. Kim, C.L. Muhlstein and R.O. Ritchie, *Mater. Sci. Eng.*, **A192/193**, 474 (1995).
9. K.T. Venkateswara Rao, Y.-W.Kim, R.O. Ritchie, *Scripta Metall. Mat.*, **33**, 495 (1995).
10. K. Badrinarayanan, A.L. McKelvey, K.T. Venkateswara Rao and R.O. Ritchie, *Metall. Mat. Trans. A*, **27**, 3781 (1996).
11. K.J. Miller, *Fat. Eng. Mater. Struct.*, **5**, 223 (1982).
12. J. Lankford, *Fat. Eng. Mater. Struct.*, **8**, 161 (1985).
13. S. Suresh and R.O. Ritchie, *Int. Metals Rev.*, **29**, 445 (1984).
14. R.O. Ritchie and J. Lankford, *Mater. Sci. Eng.*, **A84**, 11 (1986).
15. W. Elber, *Eng. Fract. Mech.*, **2**, 37 (1970).
16. R.O. Ritchie and W. Yu, in *Small Fatigue Cracks*, eds., R.O. Ritchie and J. Lankford, TMS, Warrendale, PA, 167 (1986).
17. R.O. Ritchie, W. Yu and R.J. Bucci, *Eng. Fract. Mech.*, **32**, 361 (1989).
18. J.C. Newman, Jr. and I.S. Raju, *Eng. Fract. Mech.*, **15**, 185 (1981).
19. J.P. Campbell and R.O. Ritchie, *Metall. Mat. Trans. A*, in review (1997). (available as J.P. Campbell, M.S. Thesis, University of California at Berkeley, 1996).
20. K.S. Chan, *Metall. Mat. Trans. A*, **26**, 1407 (1995).
21. K.S. Chan, *Metall. Trans. A*, **22**, 2021 (1991).
22. K.T. Venkateswara Rao, W. Yu and R.O. Ritchie, *Eng. Fract. Mech.*, **31**, 623 (1988).
23. D.L. Davidson and J.B. Campbell, *Metall. Trans. A*, **24**, 1555 (1993).
24. P. Bowen, R.A. Chave and A.W. James, *Mater. Sci. Eng. A*, **A192/193**, 443 (1995).
25. D.J. Wissuchek, G.E. Lucas and A.G. Evans, in *Gamma Titanium Aluminides*, eds. Y.-W. Kim *et al.*, TMS. Warrendale, PA, 875 (1995).
26. R. Gnanamoorthy, Y. Mutoh, K. Hayashi and Y. Mizuhara, *Scripta Metall. Mat.*, **33**, 907 (1995).